



# Unsteady mhd flow with variable viscosity: Applications of spectral scheme

M. Turkyilmazoglu

Mathematics Department, University of Hacettepe, 06532-Beytepe, Ankara, Turkey

## ARTICLE INFO

### Article history:

Received 27 July 2009

Received in revised form

7 October 2009

Accepted 20 October 2009

Available online 5 November 2009

### Keywords:

Unsteady mhd flow

Rotating disk

Variable viscosity

Chebyshev collocation

Shear stresses

Heat transfer

## ABSTRACT

The magnetohydrodynamic time-dependent von Karman swirling electrically conducting viscous fluid flow having a temperature-dependent viscosity due to a rotating disk impulsively set into motion is considered in this study. Alternative to the finite-difference methods frequently used to solve this flow, we propose here a better technique based on the spectral Chebyshev collocation in the direction normal to the disk and forward marching in time. When applied to the unsteady mhd flow in consideration, the devised numerical scheme is capable of generating the settlement of the flow into the well-known steady state for large times. The energy equation that incorporates the effects of viscous dissipation and Joule heating, and also coupled with the Navier–Stokes and continuity equations, is also treated by the method and the physical parameters of paramount interest as such the radial and tangential skin friction coefficients, the torque and the rate of heat transfer from the disk surface are numerically calculated that are shown to approach their steady state counterparts for the entire family of magnetic interaction and viscosity variation parameters.

© 2009 Elsevier Masson SAS. All rights reserved.

## 1. Introduction

A great deal of numerical solution methods has been developed recently to tackle the unsteady flow motion relevant to fluid dynamics phenomena. Due to its simplicity, finite-difference methods are generally preferred while simulating the flow field. A better technique is suggested in the present study based on the spectral Chebyshev collocation. Its advantages over the classical finite-difference methods have been highlighted with a direct application of the method to the numerical solution of the three-dimensional unsteady problem of rotating disk von Karman fluid flow having a temperature-dependent viscosity with the hydromagnetic, viscous dissipation and Joule heating effects taken into consideration.

A large class of fluid flow phenomena is described by the governing time-dependent equations of motion, see for instance [1]. The time evolution of the physical phenomenon needs to be conceived by solving numerically the fluid equations, particularly if the velocity and temperature field is not decoupled, since these equations have no analytical closed-form solutions in most cases. The governing equations generally consist of partial differential equations of mass, momentum, angular momentum and energy conservation depending on the property of the phenomenon.

Several numerical formulations based on different discretization methods, such as finite differences, finite element, and spectral methods, have been proposed to compute the fluid dynamics problems, as in the works of [2–4]. The most common approach for

approximating the derivatives is the finite-difference methods [5]. Different types and orders of finite-difference methods are available as cited in the book [6]. Applying conventional first-order finite-difference methods like the first-order upwind results in monotonic and stable solutions, but they are also strongly dissipative causing the solution of the strongly convective partial differential equations to become smeared out and often grossly inaccurate. On the other hand higher-order difference methods, e.g. central, Lax-Wendroff, QUICK, etc. are less dissipative but are prone to numerical instabilities, which introduce oscillations across regions of large gradients of the variables as discussed in [7,8]. Crank–Nicolson method is a favorably popular method for solving parabolic equations because it is unconditionally stable and second order accurate [9]. One drawback of it is that it responds severely to jump discontinuities in the initial conditions or to the differences between the initial and boundary conditions with oscillations which are weakly damped and therefore may persist for a long time. A selection of methods were later presented to reduce the amplitude of these oscillations as outlined in the studies of [10–12].

The same non-physical numerical oscillations were encountered while solving the unsteady rotating disk fluid flow problems, initially posed by [13], in [14,15] using a finite difference numerical integration procedure in conjunction with the implicit Crank–Nicolson solver. It appears that the difficulty is inherent to the other unsteady flow problems in fluid mechanics, see for example [16–18]. A fast solution for this numerical problem is generally achieved by using a proper coordinate transformation as suggested by [19]. However, besides the equations to be solved getting complicated, this even

E-mail address: [turkyilm@hacettepe.edu.tr](mailto:turkyilm@hacettepe.edu.tr)

does not remedy the problem completely, since the physical domain is infinite, imposing the asymptotic conditions at a finite distance greatly affects the accuracy of the numerical solution, as pointed out in the research of [14,20]. Therefore, the existing numerical procedures in the literature for the unsteady calculations do the computations in the transformed region up to a predetermined finite time and switches back to the physical domain for the calculation of the rest of the solution in the time domain.

The prime objective of the current work is to present a numerical scheme for the unsteady mhd flow problem as set out in [15]. A straightforward approach is the essential target of the study which easily overcomes the aforementioned difficulties and particularly avoids the unwanted numerical oscillations due to the differences between the initial and boundary conditions. To serve to this purpose, Chebyshev polynomials are employed to approximate derivatives in the direction normal to the body surface. Having linearized the nonlinear terms in the governing equations via the usual Newton linearization, the spectral collocation implemented in this way is then furnished with an implicit time differencing for the unsteady terms in the governing equations. The method is later used to solve the magnetohydrodynamic von Karman swirling flow equations governing the motion of the unsteady incompressible and conducting viscous fluid flow over a rotating disk possessing a temperature-dependent viscosity. Another motivation of the present work is to investigate the influences of viscous dissipation and Joule heating terms for the considered flow, which were omitted in [15]. The continuity, Navier–Stokes and energy equations governing the velocity and temperature fields are hence strongly coupled. Numerical oscillations and diminishing of the infinite boundary for large times inherent to the finite-difference techniques are no longer present in the method devised. Finally, the time evolution of some parameters of physical importance influenced by the presence of a uniform external normally applied magnetic field, viscous dissipation and Joule heating together with the variation of viscosity with temperature has been obtained using the current method.

The following procedure is adopted in the rest of the paper. The implicit spectral numerical scheme is presented in Section 2. Application of the method is implemented in Section 3 to the electrically conducting magnetohydrodynamic unsteady von Karman rotating disk fluid flow equations strongly coupled with the energy equation owing to a temperature-dependent viscosity assumption. Section 4 contains results and discussions of the numerical presentations including those of physically important parameters. Finally, conclusions are drawn in Section 5.

## 2. The numerical method

Unlike to the finite-difference techniques as employed in [15,21,22], we propose, for the problem at hand, a better algorithm here, known also as the fully implicit time-stepping method, see for instance [23–25]. To remind the basics of the method, we consider the system of partial differential equations,

$$\begin{aligned} \frac{\partial \mathbf{u}}{\partial t} + N_1(\mathbf{u}, T) &= 0, \\ \frac{\partial T}{\partial t} + N_2(\mathbf{u}, T) &= 0, \end{aligned} \quad (1)$$

valid inside a domain  $D$ , accompanied with the following initial and boundary conditions

$$\begin{aligned} \mathbf{u}(t = 0, z) &= \mathbf{u}_0(z), \quad T(t = 0, z) = T_0(z), \quad z \in D, \\ \mathbf{u}(t, z) &= \mathbf{a}(t), \quad T(t, z) = b(t), \quad (t, z) \in (R^+ \times \partial D), \end{aligned}$$

where  $(\mathbf{u}, T) = (u(t, z), v(t, z), w(t, z), T(t, z))$  with  $z$  being a normal coordinate in the direction perpendicular to the motion and,  $N_1$  and

$N_2$  in equations (1) are nonlinear partial differential operators akin to the Navier–Stokes and energy operators arising in many applications of science and engineering. The nonlinear terms may contain some significant parameters like the Reynolds number, Prandtl number, magnetic interaction parameter, viscosity variation parameter and so on.

There are a number of numerical procedures to discretize system (1). The most frequently used are the classical explicit or implicit finite-difference techniques. But no matter the type of the differencing, the resulting numerical algorithm gives rise to numerical oscillations due to the reason that the initial data and boundary conditions in (2) may possibly constitute a discontinuity to be exemplified later in Section 4. This fact was utterly expressed in the numerical studies of the references cited here, in which the numerical oscillations were often reported during the numerical simulation of the unsteady rotating disk flows, see for instance [14,20,15,21]. The cousins of numerical methods based on the finite-difference approximations of derivatives as presented in the book of [6] are also susceptible to the same difficulty. A solution for this numerical problem is generally accomplished by means of a proper coordinate transformation, such as

$$\eta = \frac{z}{2\sqrt{t}}, \quad (2)$$

as also suggested in [19] (notice that this transformation does preserve the semi-infinite physical domain). However, although the resulting equations need to be solved in the infinite domain

$$0 \leq z < \infty, \quad t \geq 0,$$

during the numerical computations  $z$  is fixed at a finite distance, and due to the suggested coordinate transformation in (2), this finite domain is diminished with the progression of time and greatly affects the accuracy of the numerical solution of the problem at hand. In addition to this, the transformation given in equation (2) yields nonsimilar system of equations adding both the vertical coordinate  $\eta$  and time  $t$  into the transformed equation system, with  $\eta$  tending to infinity away from the wall. One can refer to [15,20] for the transformed equations. To cope with these deficiencies, and obtain the unsteady solution at one go without introducing further nonsimilar and complicating parameters into equations, we propose here to use spectral Chebyshev method, see [4]. In compliance with this purpose, the truncated semi-infinite physical domain of computation is mapped first onto the interval  $\eta \in [-1, 1]$  with a suitable transformation  $\eta = f(z)$ . A forward time differencing for the derivative of velocity  $\mathbf{u}$  is appropriate at this stage in the form

$$\frac{\partial \mathbf{u}}{\partial t} = \frac{\mathbf{u}_{j+1} - \mathbf{u}_j}{\Delta t},$$

with a similar time discretization for the temperature  $T$ . Taking into account the advantage of fully implicit schemes, the nonlinear terms in (1) are imposed at the time  $t + \Delta t$  which results in  $N(\mathbf{u}_{j+1}, T_{j+1})$  terms being present. Next, these nonlinear terms are linearized with the usual Newton linearization technique such that the time-discrete flow velocities and temperature are written by

$$\begin{aligned} \mathbf{u}_j &= \mathbf{u}_j^{(n)} + \delta \mathbf{u}_j, \\ T_j &= T_j^{(n)} + \delta T_j \end{aligned} \quad (3)$$

where  $\mathbf{u}_j^{(n)}$  and  $T_j^{(n)}$  are to denote the values of  $\mathbf{u}_j$  and  $T_j$  at the iteration number  $n$  and,  $\delta \mathbf{u}_j$  and  $\delta T_j$  are small correction terms. Usually this method is used for steady problems, in which the process of successive approximations is continued until the relative differences of the physical quantities between two successive iterative steps are smaller than a given error. It should be remarked

that such a condition can also be set at the time increment to be evaluated with the known data picked up from the previous time step. As a result, the nonlinear operators in (1) are substituted by their linearized counterparts.

A Chebyshev collocation based on the well-known Chebyshev polynomials is later employed in the wall normal direction  $\eta$  in such a way that the quantities are collocated at the Gauss points

$$\cos\left(\frac{k\pi}{N}\right), \quad k = 0, 1, \dots, N,$$

where  $N$  denotes the number of collocation points used. The spectral Chebyshev collocation method enables one also to represent a derivative of a quantity in terms of the values of that quantity in the whole domain of interest, see [4]. In view of the above remarks, system (1) can be cast into a matrix form

$$\mathbf{A}\delta\mathbf{U}_{j+1} = \mathbf{R}, \quad (4)$$

in which  $\mathbf{A}$  ( $(4N+4) \times (4N+4)$  square matrix) and  $\mathbf{R}$  ( $(4N+4) \times 1$  column vector) consist of the known values at the  $n$ th iteration, and  $\delta\mathbf{U}_{j+1}$  is an  $(4N+4) \times 1$  column vector showing the corrections at the instant of computation for  $(u, v, w, T)$ . The matrix system (4) needs to be modified due to the boundary constraints (2). With proper initial approximations  $\mathbf{u}^{(n)}$  to the variables (which can be assigned from the previously converged solutions) at each time step, the sparse matrix system (4) is eventually solved with an  $LU$  matrix factorization technique. The convergence criterion is to force the correction terms  $\delta\mathbf{U}$  in (4) to lie within a preassigned small tolerance.

More details of the integration scheme without the time derivatives (steady state) can be found in [26]. We should emphasize that the initial guesses mentioned above are taken as zero initially, which were found to be perfectly capable of generating the results of this study for the entire family of parameters considered.

### 3. Formulation of the problem

The concern here is with the three-dimensional, unsteady mhd flow of an incompressible, viscous electrically conducting fluid over an infinite disk rotating with a constant angular velocity  $\Omega$  about its axis of rotation  $z$ . The flow is influenced by the presence of an externally applied uniform normal magnetic field. The governing equations of motion are non-dimensionalized with respect to a length scale  $L = r_e^*$ , velocity scale  $U_c = L\Omega$ , time scale  $L/U_c$  and pressure scale  $\rho U_c^2$ , where  $\rho$  is the fluid density. Such a dimensionless analysis leads to a global Reynolds number  $Re = (U_c L)/\nu = R^2$ , where  $R$  is the Reynolds number based on the displacement thickness  $\delta = (\nu/\Omega)^{1/2}$ ,  $\nu$  being the kinematic viscosity. Thus, relative to the non-dimensional cylindrical polar coordinates  $(r, \theta, z)$ , the full time-dependent, continuity, Navier–Stokes, energy and generalized Ohm's law equations governing the conducting viscous fluid flow are given by,

$$\nabla \cdot \mathbf{u} = 0, \quad (5)$$

$$\frac{\partial \mathbf{u}}{\partial t} + (\mathbf{u} \cdot \nabla) \mathbf{u} = -\nabla p + \frac{1}{R^2} \nabla \cdot (\mu \nabla \mathbf{u}) + \mathbf{J} \times \mathbf{B}, \quad (6)$$

$$\frac{\partial T}{\partial t} + \mathbf{u} \cdot \nabla T = \frac{1}{Pr R^2} \nabla^2 T + Ec \frac{\mu}{r^2 R^2} [u_z^2 + v_z^2] + Ec \frac{M}{r^2} [u^2 + v^2], \quad (7)$$

$$\mathbf{J} = \sigma [E + \mathbf{u} \times \mathbf{B}]. \quad (8)$$

The present analysis assumes that the fluid lies in the  $z \geq 0$  semi-infinite space. In the above equations (5)–(8),  $\nabla^2$  is the usual Laplacian operator in cylindrical coordinates. It should be noted that the viscous dissipation and Joule heating effects are taken into account in

the energy equation (7), which were disregarded in the study of [15].  $Pr = (\mu_\infty c_p)/\kappa_\infty$  is the Prandtl number,  $Ec = r^2/c_p(T_w - T_\infty)$  is the Eckert number (we define it like this, since it is related to the Eckert number found in the heat transfer literature),  $c_p$  is the specific heat at constant pressure,  $\kappa$  is the thermal conductivity ( $\infty$  denoting a free-stream value). The components of the flow velocity  $\mathbf{u}$  are  $(u, v, w)$ , the pressure is  $p$  and  $T$  is the fluid temperature such that the surface of the rotating disk is maintained at a uniform temperature  $T_w$ . Far away from the wall, the free stream is kept at a constant temperature  $T_\infty$ . As for the velocities, no-slip condition is imposed at the wall together with the vanishing radial and azimuthal velocities far above the disk.

The fluid is assumed to be Newtonian, viscous and electrically conducting. The external uniform magnetic field  $\mathbf{B}$  is applied perpendicular to the surface of the disk and has a constant magnetic flux density  $B_0$  which is assumed unchanged by taking small magnetic Reynolds number  $R_m = \sigma \mu L^2 \Omega$ , much smaller than the Reynolds number of the fluid, which is the case for several practical situations and  $\sigma$  the electrical conductivity of the fluid. Thus, the applied magnetic field is unaffected by the effect of the motion of the conducting fluid, due to the low magnetic Reynolds number assumption. Whereas, the effect of the magnetic field on the hydrodynamic properties of the fluid motion manifests itself in the form  $\mathbf{J} \times \mathbf{B}$  on the right hand side of the momentum equations (2). This is known as, the Lorentz force, the components of whose can be evaluated as  $M(-u, -v, 0)$  for a normal electric field with  $M$  the magnetic interaction parameter positive and defined by  $M = (\sigma B_0^2)/\rho \Omega$ . It is further assumed that there are no radial or azimuthal currents influencing the motion of the fluid flow under consideration.  $E$  is the electric field which results from charge separation and is in the  $z$ -direction. It should be noticed that the electric field does not influence the motion.

In addition, instead of a constant viscosity of the fluid, we assume that the viscosity depends on the temperature, that is  $\mu = 1/(1 + \varepsilon(T - T_\infty)/(T_w - T_\infty))$  as in the works of [15,27].  $\varepsilon$  is termed the viscosity variation parameter. All other material functions are treated as constant. However, it is known that viscosity may change significantly with the temperature and therefore viscosity variations should be taken into consideration to accurately resolve the flow field, as is the case for the convection problems, see for instance [22,21].

The dimensionless mean flow velocities, pressure and temperature distributions are given by von Karman's exact self-similar solution of the Navier–Stokes equations for the steady laminar flow in the case of nonconducting fluid. A similar argument holds here for the conducting flow equations, too. Because the boundary layer thickness is of order of magnitude  $R^{-1}$ , the steady incompressible boundary layer flow over a rotating disk evolves along a boundary layer coordinate of order unity, defined by  $Z = Rz$ . Consequently, the mean flow quantities take the form,

$$\begin{aligned} (u, v, w) &= (rF(t, Z), rG(t, Z), \frac{1}{R}H(t, Z)), \\ (p, T) &= \left( \frac{1}{R^2}\bar{P}(t, Z), T_\infty + (T_w - T_\infty)\theta(t, Z) \right), \end{aligned} \quad (9)$$

where the similarity functions  $F, G, H$  and  $\theta$  satisfy the following ordinary differential equations

$$\begin{aligned} \frac{\partial F}{\partial t} - (\Phi F')' + F^2 - G^2 + F'H + MF &= 0, \\ \frac{\partial G}{\partial t} - (\Phi G')' + 2FG + G'H + MG &= 0, \\ \frac{\partial \bar{P}}{\partial t} - (\Phi H')' + P' + H'H &= 0, \\ 2F + H' &= 0, \\ \frac{\partial \theta}{\partial t} - \frac{1}{Pr} \theta'' + H\theta' - Ec\Phi[F'^2 + G'^2] - EcM[F^2 + G^2] &= 0. \end{aligned} \quad (10)$$

The last two terms in the last equation in system (10) stem from the viscous dissipation and Joule heating effects, respectively. Moreover, a prime denotes derivative with respect to  $Z$ ,  $\Phi = 1/1 + \varepsilon\theta$  and the boundary conditions appropriate to the flow geometry for all time  $t$  are given as,

$$\begin{aligned} F = G - 1 = H = \theta - 1 = 0, & \quad \text{at } Z = 0, \\ F = G = \theta = 0, & \quad \text{as } Z \rightarrow \infty. \end{aligned} \quad (11)$$

System is also supplemented with the subsequent initial values valid for all  $Z$ ,

$$F = G = H = \theta = 0, \quad \text{at } t = 0. \quad (12)$$

It should be noticed that, as stated before, a discontinuity is present between initial values and boundary conditions in (11) and (12). A nonsimilar counterpart of the system (10)–(12) was obtained in [15] using a transformation similar to (2). However, the nonsimilarity equations (see equations (11–15) in [15]) get complicated as compared to the system obtained here, which is more convenient in terms of a numerical treatment.

Upon solution of the mean flow quantities from the system (10)–(12), the skin friction coefficients, the torque and the rate of heat transfer to the surface, which are of principal physical interest, can also be calculated. The action of the viscosity in the fluid adjacent to the disk sets up a tangential shear stress, which opposes the rotation of the disk. As a consequence, it is necessary to provide a torque at the shaft to maintain a steady rotation. To find the tangential shear stress  $\tau_\theta$  and radial shear stress  $\tau_r$ , we apply the Newtonian formulae,

$$\begin{aligned} \tau_\theta &= \left[ \mu \left( \frac{\partial v}{\partial z} + \frac{1}{r} \frac{\partial w}{\partial \theta} \right) \right]_{z=0} = \Omega \frac{R}{1 + \varepsilon} G'(0), \\ \tau_r &= \left[ \mu \left( \frac{\partial u}{\partial z} + \frac{\partial w}{\partial r} \right) \right]_{z=0} = \Omega \frac{R}{1 + \varepsilon} F'(0). \end{aligned} \quad (13)$$

The rate of heat transfer from the disk surface to the fluid is computed by the application of Fourier's law as given below,

$$q = -\kappa \frac{\partial T}{\partial z} \Big|_{z=0} = -R\theta'(0), \quad (14)$$

from which the normalized Nusselt number can be obtained. Therefore, in what follows we numerically compute  $F'(0)$ ,  $G'(0)$  and  $\theta'(0)$  to understand the underlying physics of the problem.

#### 4. Results and discussion

The numerical scheme described in Section 2 was made use for the resolution of the velocity and temperature fields from the system of equations (10)–(12), after mapping the computational domain  $[0, Z_{\max}]$  onto  $\eta \in [-1, 1]$  via the linear transformation  $\eta = -1 + 2(Z/Z_{\max})$ . Sufficient number of Gauss collocation points were taken together with the proper choice of a large distance  $Z_{\max}$  above the surface of the disk in order to make sure that the solutions obtained are independent of the parameters involved. Numerical simulations are carried out for the motion of a fluid

having Prandtl number  $Pr = 1$  for an ideal flow and  $Pr = 0.72$  for air with a variety of viscosity variation parameter  $\varepsilon$  and magnetic interaction parameter  $M$ . Time progression of the unsteady velocity profiles as well as radial and tangential shear stresses, vertical suction velocity and the rate of heat transfer at the disk surface are presented against the time.

Numerical values of  $F'(0)$ ,  $G'(0)$ ,  $H(\infty)$  and  $\theta'(0)$  for the nonmagnetic flow corresponding to several values of  $\varepsilon$  are presented in Table 1. The computations are for  $Pr = 0.72$  without the viscous dissipation effects. The tabulated values were obtained from the converged large time limit of time-dependent flow as well as the corresponding steady state flow. These are compared with those steady state calculations of [27] for the fixed collocation numbers  $N = 64$  and  $Z_{\max} = 20$ . An excellent agreement can be observed, pointing to the achievement of our numerical procedure without any numerical difficulties as compared to the finite-difference techniques for the flow considered.

Starting from the zero initial state, the ideal flow over a disk evolves impulsively by a sudden action of rotation of the disk and as time passes the flow settles down to a steady state. This action of the fluid flow is shown in Fig. 1a–d for a nonmagnetic disk and in Fig. 2a–d for a magnetic ( $M = 1$ ) disk respectively without the viscous dissipation and Joule heating effects. Figures are displayed for the time development of the flow quantities by a time step  $\Delta t = 0.05$ , but taken at a snapshot of  $t = 0.5$ . The sufficiently large time solution as well as the steady solution are shown by the dot-dashed curves. Figures show how the impulsive motion ends up with a steady state which were calculated by ignoring the time derivative terms in equations (10)–(12). The success of the devised numerical method in capturing the steady state solution by assigning larger time steps is also possible (though not demonstrated here) due to its unconditional stability. It is further noticeable from the figure that the circumferential velocity attains its steady state quickest as compared to the other physical variables. It is no surprising to witness that the magnetic field helps the velocities to reach their asymptotic limit faster, whereas it delays the attendance for the temperature field due to the well-known increasing temperature impact of magnetic field. It can also be observed from Figs. 1 and 2a–d that the physical steady state is reached in a self-similar manner.

We demonstrate in Figs. 3 and 4a–d the time development of  $F'(0)$ ,  $-G'(0)$ ,  $H(\infty)$  and  $-\theta'(0)$ , respectively for the nonmagnetic and magnetic cases ( $M = 1$ ) with  $Ec = 0$ , which are closely related to the radial skin friction, azimuthal skin friction (also torque), axial velocity at infinity and the local rate of heat transfer for  $Pr = 0.72$  and all computed with a step size of  $\delta t = 0.01$ . The steady state values are also shown by the broken lines in the figure. It can again be seen that the method successfully generates the steady state values of the physically important parameters, the fastest for the case of tangential skin frictions consistent with Figs. 1 and 2. Figs. 3 and 4a–d demonstrate that increasing the magnetic field strength decreases the heat transfer rates from the surface of the disk. Moreover, an increase in the viscosity variation parameter  $\varepsilon$  is associated with the enhancement of the radial skin friction coefficient  $F'(0)$  and vertical wall suction  $H(\infty)$ , a reverse effect is observed for the azimuthal skin friction coefficient and heat transfer. Thus we may conclude that the physical effect of viscosity parameter on the skin friction is twofold.

**Table 1**

The values of  $F'(0)$ ,  $G'(0)$ ,  $H(\infty)$  and  $\theta'(0)$  ranging from  $\varepsilon = 0$  to  $\varepsilon = 6$  for the nonmagnetic flow case. <sup>1</sup> and <sup>2</sup> respectively refer to our results and those of [27].

$\varepsilon$	$F'(0)^1$	$G'(0)^1$	$H(\infty)^1$	$\theta'(0)^1$	$F'(0)^2$	$G'(0)^2$	$H(\infty)^2$	$\theta'(0)^2$
0	0.510232	−0.615922	−0.884473	−0.328574	0.5102	−0.6159	−0.8844	−0.3285
2	0.883388	−1.109708	−0.286650	−0.595032	0.8833	−1.1097	−0.2866	−0.5950
4	1.140804	−1.421316	−0.249492	−0.448758	1.1408	−1.4213	−0.2494	−0.4487
6	1.350172	−1.670884	−0.221672	−0.368288	1.3501	−1.6708	−0.2216	−0.3682

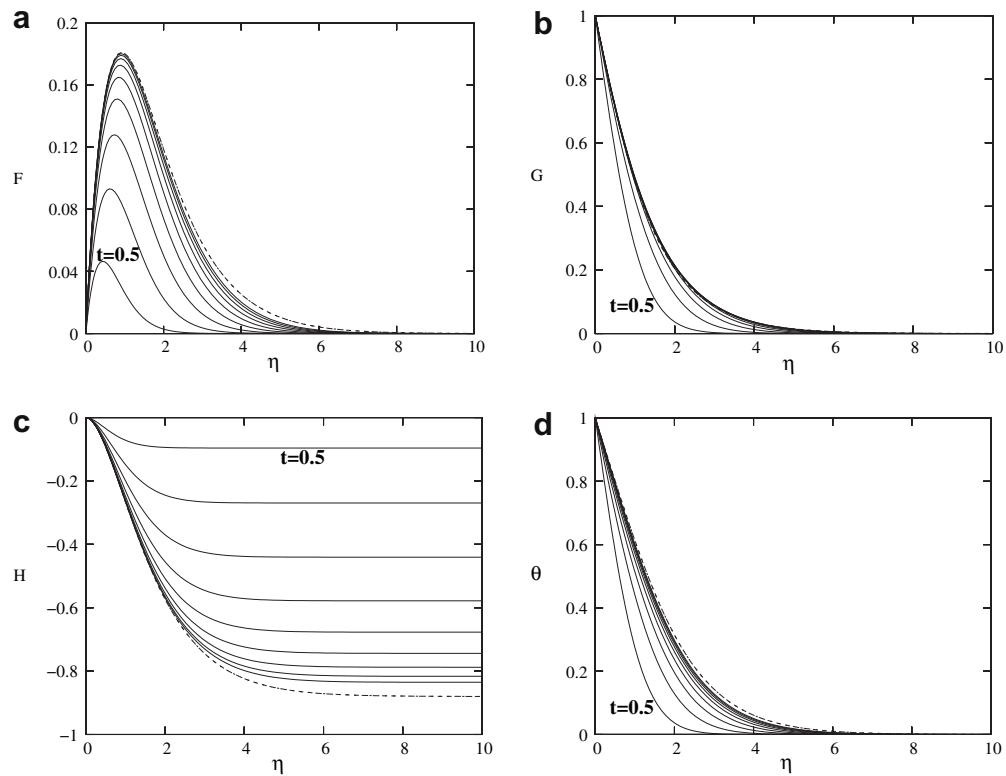


**Fig. 1.** The time progression of basic flow quantities for the rotating disk flow are shown for a nonmagnetic and constant viscosity case with  $Ec = 0$  respectively in (a) the radial velocity profiles, (b) the circumferential velocity profiles, (c) the wall normal velocity profiles and (d) the temperature profiles. The snapshots are given at 0.5 increments in time. The dot-dashed curves correspond to the large time limit as well as the steady solution.

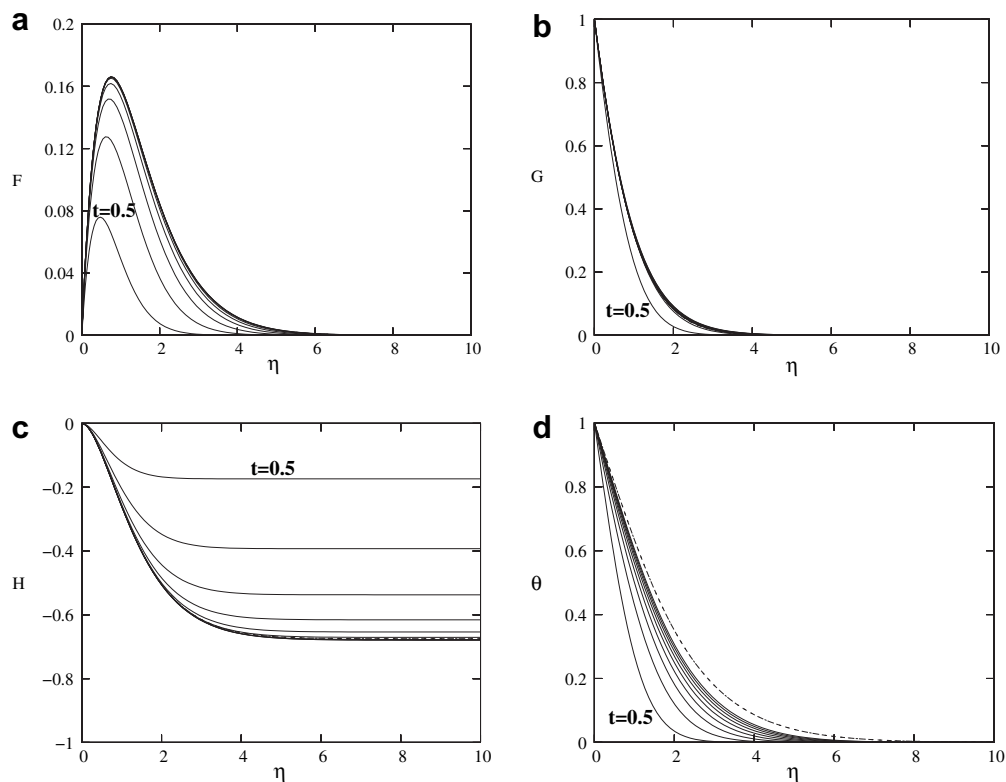


**Fig. 2.** The time progression of basic flow quantities for the rotating disk flow are shown for a magnetic ( $M = 1$ ) and constant viscosity parameter case with  $Ec = 0$  respectively in (a) the radial velocity profiles, (b) the circumferential velocity profiles and (d) the temperature profiles. The snapshots are given at 0.5 increments in time. The dot-dashed curves correspond to the large time limit as well as the steady solution.



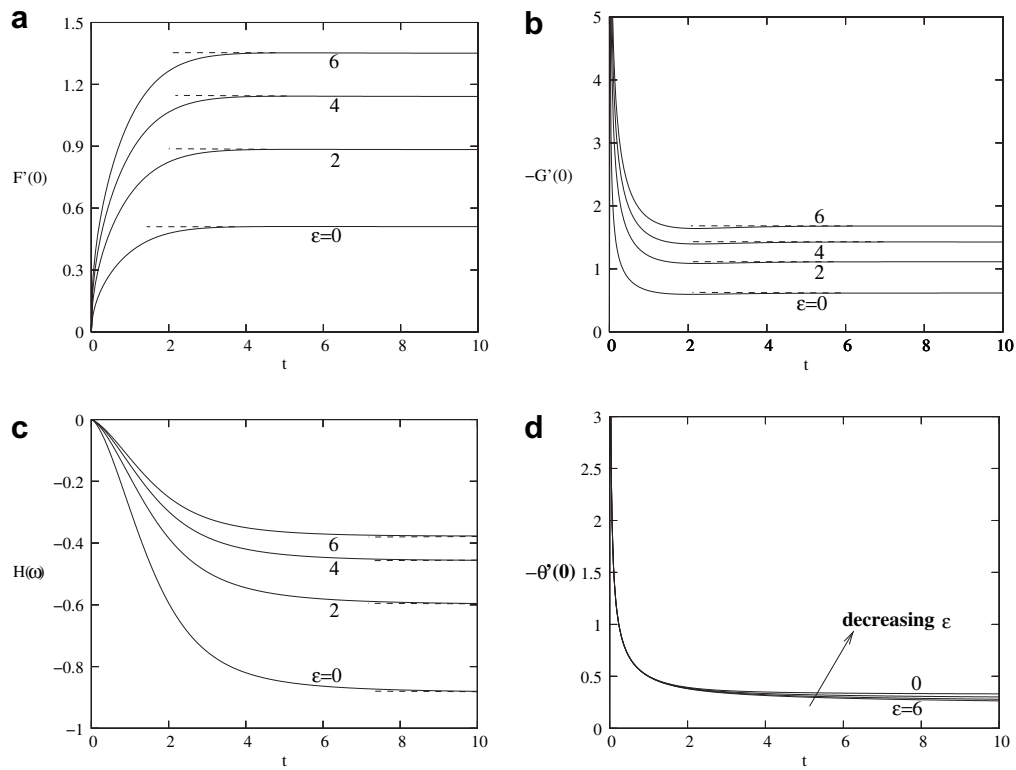


**Fig. 3.** The time progression of physically significant parameters are shown for the nonconducting flow case with  $Ec = 0$  respectively in (a)  $F'(0)$ , (b)  $-G'(0)$ , (c)  $H(\infty)$  and (d)  $-\theta'(0)$ . A dashed line corresponds to the steady state value.

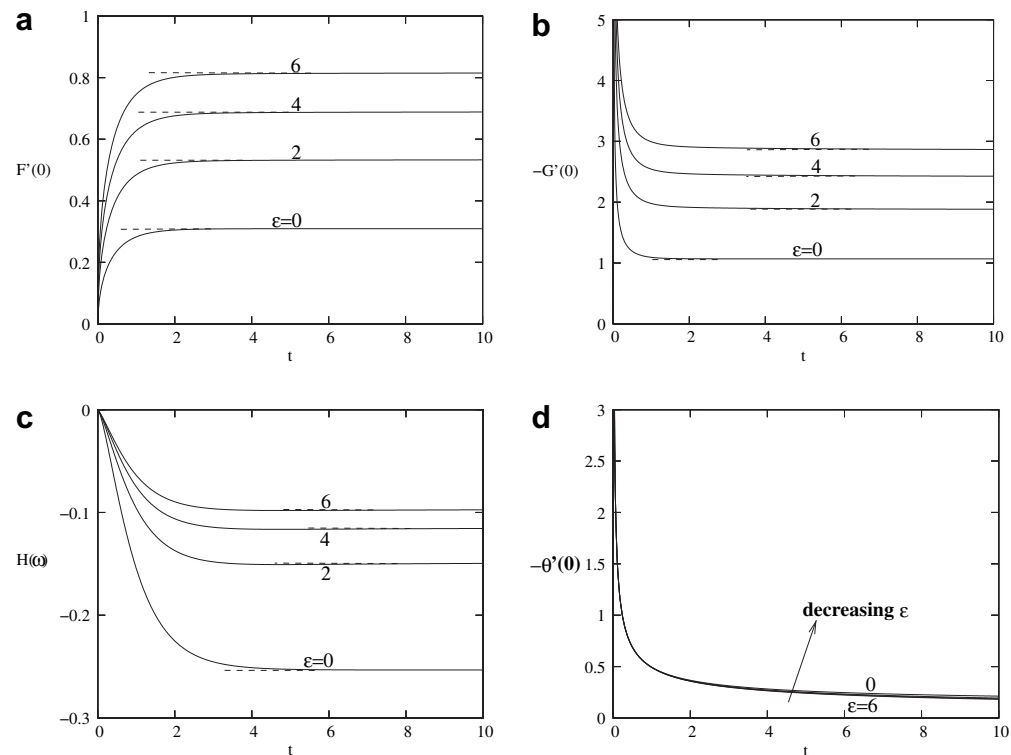


**Fig. 4.** The time progression of physically significant parameters are shown for the conducting flow case with  $M = 1$  and  $Ec = 0$  respectively in (a)  $F'(0)$ , (b)  $-G'(0)$ , (c)  $H(\infty)$  and (d)  $-\theta'(0)$ . A dashed line corresponds to the steady state value.

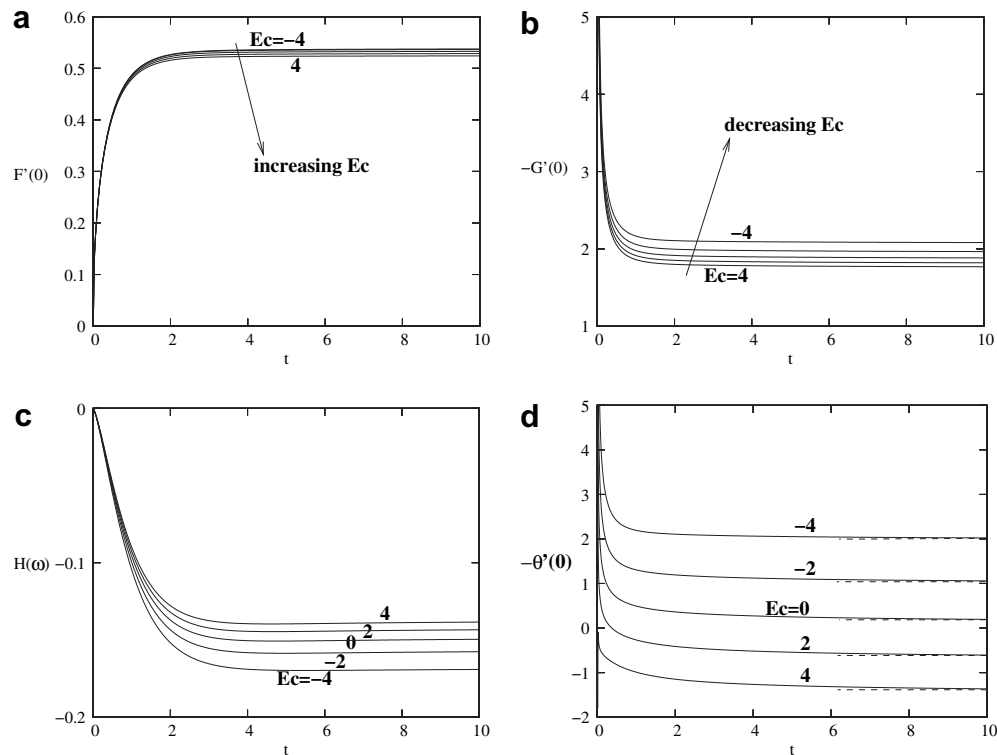


**Fig. 5.** The time progression of physically significant parameters are shown for the conducting flow case with  $M = 1$  and  $\varepsilon = 2$  respectively in (a)  $F'(0)$ , (b)  $-G'(0)$ , (c)  $H(\infty)$  and (d)  $-\theta'(0)$ . A dashed line corresponds to the steady state value.

Influences of viscous dissipation and Joule heating terms are shown finally in Fig. 5a–d on the considered flow and heat transfer characteristics for the selected parameters  $M = 1$  and  $\varepsilon = 2$  for various values of  $Ec$ . It is seen that influences are more profound on the temperature profiles as compared to the velocity field. Increasing  $Ec$  results in an increase in both the axial velocity and the azimuthal skin friction parameter, whereas it results in a decrease in both the radial skin friction parameter and the rate of heat transfer. On the other hand, just an opposite scenario takes place for values of  $Ec$  decreasing. Thus, we conclude that the inclusion of viscous dissipation and Joule heating in the energy equation can significantly alter the physical character of the flow quantities and heat transfer.

## 5. Conclusions

The three-dimensional unsteady magnetohydrodynamic boundary layer flow due to a rotating disk with the viscous dissipation and Joule heating also in effect has been considered in the present work. Opposite to the finite-difference techniques more often used in the literature, a better numerical integration scheme has been proposed here. The method is based on the spectral Chebyshev collocation discretization along the coordinate normal to the fluid flow motion and Euler implicit forward time discretization in time, known also the fully implicit time-stepping method. The electrically conducting mean velocity and temperature fields, under the influence of a temperature-dependent viscosity, approaching their steady states have been successfully computed with this method. We have presented results to illustrate the flow characteristics for the velocity and temperature fields as well as the skin friction and rate of heat transfer, and show how the flow fields are influenced by the material parameters of the flow problem.

The presented fully implicit spectral technique can resolve the discontinuities occurring due to the different initial and boundary

conditions in an unsteady flow motion. Using the numerical method, the incompressible, viscous, laminar and time-dependent hydro-magnetic three-dimensional swirling conducting fluid flow over a rotating disk subject to a variable property of viscosity has been solved. The viscous dissipation and Joule heating terms have also been retained in the energy equations. Starting from zero initial solutions and advancing in time, the method successfully generates the velocity and temperature distributions influenced by the existence of a magnetic field of the other parameters considered and evolve into their steady state counterparts after a sufficient time past. The numerical results have been initially validated by comparing them with the available results in the literature in the nonmagnetic and steady state case without the viscous dissipation and Joule heating impacts. Excellent agreements have been found for all the parameters of physical importance. The torque, shear stresses, axial suction velocity and heat transfer rate, which are of fundamental importance in view of physics, have next been calculated with varying magnetic interaction and viscosity variation parameters as well as Prandtl and Eckert numbers. Increasing magnetic field strength decreases the wall shear stress, rate of heat transfer and hence the magnetic field significantly controls the flow and heat characteristics. Results have also shown that the rate of heat transfer is sensitive to the physical parameters under consideration, and all other parameters fixed under the influence of viscous dissipation, decreasing the Eckert number has been found to enhance the rate of heat transfer, with an opposite effect for increasing Eckert numbers.

## References

- [1] H. Schlichting, *Boundary-Layer Theory*, McGraw-Hill, 1979.
- [2] H. Fasel, Investigation of the stability of boundary layers by a finite-difference model of the Navier–Stokes equations. *J. Fluid Mech.* 78 (1976) 355–383.

- [3] C. Basdevant, M. Deville, P. Haldenwa, J.M. Lacroix, J. Quazzani, R. Peyret, P. Orlandi, A.T. Patera, Spectral and finite-difference solutions of burgers-equation. *Comput. Fluids* 14 (1986) 23–41.
- [4] C. Canuto, M.Y. Hussaini, A. Quarteroni, T.A. Zang, *Spectral Methods in Fluid Dynamics*. Springer-Verlag, 1988.
- [5] R.D. Richtmyer, K.V. Morton, *Difference Methods for Initial Value Problems*. Interscience, 1967.
- [6] D.L. Book, *Finite Difference Techniques for Vectorized Fluid Dynamics Calculations*. Springer-Verlag, 1981.
- [7] J.D. Hoffman, *Numerical Methods for Engineering and Scientists*. McGraw-Hill, 1993.
- [8] Y. Wang, K. Hutter, Comparison of numerical methods with respect to convectively dominated problems. I. *J. Num. Meth. Fluids* 37 (2001) 721–745.
- [9] J. Crank, P. Nicolson, A practical method for numerical evaluation of solutions of partial differential equations of the heat-conduction type. *Proc. Camb. Phil. Soc.* 43 (1947) 50–67.
- [10] H.C. Yee, Construction of explicit and implicit symmetric tvd schemes and their applications. *J. Comput. Phys.* 68 (1987) 151–179.
- [11] W. Shyy, M.H. Chen, R. Mittal, H.S. Udaykumar, On the suppression of numerical oscillations using a non-linear filter. *J. Comput. Phys.* 102 (1992) 49–62.
- [12] D. Britz, O. Qsterby, J. Strutwolf, Damping of Crank–Nicolson error oscillations. Submitted *Comput. Chem.* (2002).
- [13] E.T. Benton, On the flow due to a rotating disk. *J. Fluid Mech.* 24 (1966) 781–800.
- [14] H.A. Attia, Unsteady mhd flow near a rotating porous disk with uniform suction or injection. *Fluid Dyn. Res.* 23 (1998) 283–290.
- [15] M.A. Hossain, A. Hossain, M. Wilson, Unsteady flow of viscous incompressible fluid with temperature-dependent viscosity due to a rotating disc in the presence of transverse magnetic field and heat transfer. *Int. J. Therm. Sci.* 40 (2001) 11–20.
- [16] W.J. Minkowycz, Sparrow, Numerical solution scheme for local non-similarity boundary layer analysis. *Numer. Heat Transfer* 1 (1978) 69–85.
- [17] J. Gary, D.R. Kassory, H. Tadjeran, A. Zebib, The effect of significant viscosity variation on convective heat transport in water-saturated porous media. *J. Fluid Mech.* 117 (1982) 233–249.
- [18] K.N. Mehta, S. Sood, Transient free convection flow with temperature dependent viscosity in fluid saturated porous medium. *Int. J. Eng. Sci.* 30 (1992) 1083–1087.
- [19] W.F. Ames, *Numerical Methods in Partial Differential Equations*. Academic Press, 1977.
- [20] H.A. Attia, Time varying rotating disk flow and heat transfer of a conducting fluid with suction or injection. *Int. Comm. Heat Mass Transfer* 30 (2003) 1041–1049.
- [21] M.A. Hossain, S. Kabir, D.A.S. Rees, Natural convection of fluid with variable viscosity from a heated vertical wavy surface. *Z. Angew. Math. Phys.* 53 (2002) 48–57.
- [22] N.G. Kafoussias, D.A.S. Rees, Numerical studies of the combined free and forced convective laminar boundary layer flow past a vertical isothermal flat plate with temperature-dependent viscosity. *Acta Mech.* 127 (1998) 39–50.
- [23] J. Kim, P. Moin, On the numerical solution of time-dependent viscous incompressible fluid flows involving solid boundaries. *J. Comput. Phys.* 35 (1980) 381–392.
- [24] M.Y. Hussaini, T.A. Zang, Spectral methods in fluid dynamics. *Ann. Rev. Fluid Mech.* 19 (1987) 339–367.
- [25] R.D. Joslin, C.L. Street, C.L. Chang, Validation of three-dimensional incompressible spatial direct numerical simulation code. *NASA Tech. Note No. 3205* (1992) 1–18.
- [26] M. Turkyilmazoglu, Linear absolute and convective instabilities of some two- and three dimensional flows, PhD Thesis, University of Manchester, 1998.
- [27] H.A. Jasmine, J.S.B. Gajjar, Absolute and convective instabilities in the incompressible boundary layer on a rotating disk with temperature-dependent viscosity. *I.J. Heat Mass Trans.* 48 (2005) 1022–1037.